

Mapping sources, sinks, and connectivity using a simulation model of northern spotted owls

Nathan H. Schumaker · Allen Brookes · Jeffrey R. Dunk · Brian Woodbridge · Julie A. Heinrichs · Joshua J. Lawler · Carlos Carroll · David LaPlante

Received: 19 June 2013 / Accepted: 3 February 2014 / Published online: 23 February 2014
© Springer Science+Business Media Dordrecht (outside the USA) 2014

Abstract Source-sink dynamics are an emergent property of complex species–landscape interactions. A better understanding of how human activities affect source-sink dynamics has the potential to inform and improve the management of species of conservation concern. Here we use a study of the northern spotted owl (*Strix occidentalis caurina*) to introduce new methods for quantifying source-sink dynamics that simultaneously describe the population-wide consequences of changes to landscape connectivity. Our spotted owl model is mechanistic, spatially-explicit, individual-based, and incorporates competition with barred owls (*Strix varia*). Our observations of spotted owl source-sink dynamics could not have been inferred solely from habitat quality, and were sensitive to landscape connectivity and the spatial sampling schemes employed by the model. We conclude that a clear understanding of source-sink dynamics can best

be obtained from sampling simultaneously at multiple spatial scales. Our methodology is general, can be readily adapted to other systems, and will work with population models ranging from simple and low-parameter to complex and data-intensive.

Keywords HexSim · Habitat connectivity · Net flux · Population viability analysis

Introduction

When models are used in conservation planning, there will be tension between the drive for ever-increasing realism, and caution inspired by an awareness of the liabilities associated with model complexity. More sophisticated models can account for realistic real-world interactions (Koh et al. 2013; Kool et al. 2013), for example the impacts that climate change (e.g.

N. H. Schumaker (✉) · A. Brookes
U.S. Environmental Protection Agency,
200 SW 35th Street, Corvallis, OR 97333, USA
e-mail: nathan.schumaker@gmail.com

J. R. Dunk
Department of Environmental Science and Management,
Humboldt State University, 1 Harpst St., Arcata,
CA 95521, USA

B. Woodbridge
US Fish and Wildlife Service, Yreka Fish and Wildlife
Office, 1829 South Oregon Street, Yreka, CA 96097, USA

J. A. Heinrichs · J. J. Lawler
School of Environmental and Forest Sciences, University
of Washington, 352100, Seattle, WA 98195, USA

C. Carroll
Klamath Center for Conservation Research,
747 Ishi Pishi Road, Orleans, CA 95556, USA

D. LaPlante
Natural Resources Geospatial, 207 Ridgeview Drive,
Montague, CA 96064, USA

Núñez et al. 2013) may have on a population that is already responding to habitat loss and fragmentation (e.g. Ferraz et al. 2007), and competition (e.g. Wiens 2012). But realism comes at a cost, as complex models are harder to understand, parameterize, and defend (Minor et al. 2008; Hudgens et al. 2012).

The incorporation of source-sink dynamics into population models illustrates this trade-off. We know from past work (Pulliam 1988; Liu et al. 2011) that demographic sources are important for population stability, but that sinks can play a critical role as stepping stones for long distance dispersal, or by increasing the likelihood that extirpated sites become recolonized. Identifying and quantifying the value of individual source and sink areas to a population is becoming an important objective in conservation research and planning (Hansen 2011; Jacobi and Jonsson 2011). But meeting this goal is difficult because it involves estimating occupancy rates, movement rates, and landscape connectivity (Goodwin 2003; Baguette and Van Dyck 2007; Moilanen 2011; Rayfield et al. 2011; Koh et al. 2013; Kool et al. 2013). Simulation models can help, but those having the capacity to perform such assessments tend to be complex.

The most popular current approaches to quantifying landscape connectivity involve applications of graph theory (Bunn et al. 2000), circuit theory (McRae et al. 2008), and network flow (Phillips et al. 2008). These innovations are inspiring the creation of parsimonious management-relevant models. But thus far, these methods also require that landscape structure and species' life histories be greatly simplified. Here we develop a complementary approach that can simulate source-sink dynamics and connectivity using as little or as much ecological detail as is deemed appropriate.

In 1990, the northern spotted owl (*Strix occidentalis carina*) was designated a threatened species under the United States' Endangered Species Act (USFWS 1990). At that time, northern spotted owl (NSO) population declines were primarily attributed to habitat loss (Thomas et al. 1990; McKelvey et al. 1993; Noon and McKelvey 1996). Nearly half of the NSO's geographic range falls within public lands, and political pressure associated with the granting of legal status contributed to the creation of the Northwest Forest Plan (USDA and USDI 1994), which helped stem the loss of habitat by nearly doubling the amount of federal land in habitat reserves. Since the NSO's

initial listing, a congener, the barred owl (*S. varia*) has gone from being worrisome (Courtney et al. 2004), to become a significant factor complicating NSO management (Dugger et al. 2011; Forsman et al. 2011; USFWS 2011; Wiens 2012; Yackulic et al. 2012). Barred owl (BO) impacts are unevenly distributed throughout the NSO's 20 million ha geographic range, and the BO is probably still in the midst of a range expansion (Forsman et al. 2011; USFWS 2011—Appendix B).

The fundamental challenges to NSO conservation are not unique, but the species stands out because enough is known about it to make the development of complex demographic models possible. We make use of a detailed NSO model here, but do so for the purpose of introducing new methodology—our intent is not to design, improve, or promote NSO management strategies. We begin with the construction of a mechanistic, spatially-explicit, individual-based model (IBM). Then, using output from the IBM, we assemble matrix models, and use them to characterize landscape connectivity and NSO source-sink dynamics.

Methods

Study region

The U.S. range of the NSO extends from northern California to the top of Washington state, and our NSO simulations spanned this area. We made use of a static map of NSO habitat quality, plus other spatial data that captured additional features relevant to the simulation model (see below). A small population of NSOs exists in British Columbia, Canada, but our study did not include this portion of the owl's range.

Simulation model

We used HexSim (Heinrichs et al. 2010; Stronen et al. 2012; Marcot et al. 2013; Schumaker 2013) to construct a population model for the NSO. HexSim is a spatially-explicit, individual-based simulation framework used to construct models of plant and animal population dynamics and interactions. HexSim models are built around a user-defined life cycle consisting of a sequence of events including survival, reproduction, movement, resource acquisition, species interactions and more. Each simulated individual

possesses traits that can vary probabilistically based on genotype, or in response to age, resource availability, disturbance, and competition. Thus individual attributes may change in time and space.

The simulation model used here was developed as part of the most recent US Fish and Wildlife Service recovery planning process for the NSO (USFWS 2011). Simulations began with 10,000 females placed into the best habitats throughout the landscape (males were not modeled). A large starting population ensured that the simulated NSOs were initially well-distributed throughout their range. We included impacts of BOs on NSO survival rates, but did not simulate BOs explicitly. Our principal results were gathered from 10 replicate simulations of 1,000 time-steps. Each time step was the equivalent of a single year, but since our landscape conditions were static, these simulations should not be construed as making projections far into the future. Data other than population size were gathered from time steps 500–1,000, well after the perturbations resulting from initial conditions had subsided. Equivalent results could have been obtained using larger numbers of shorter replicates. Our approach (more time steps, fewer replicates) was computationally efficient as the simulations ran slowly prior to reaching steady state. These 10 principal replicate simulations did not include environmental stochasticity; however, a companion set of 100 replicates were conducted that did. These additional model runs made it possible to examine how variability in the model parameters affected our results.

Spatial data

HexSim represents space as an array of hexagonal cells, and while these spatial data may be temporally dynamic, only static maps were used in this study. Our NSO model made use of three such input maps describing NSO habitat conditions (circa 2006), 11 distinct modeling regions (USFWS 2011), and 12 physiographic provinces. The map of physiographic provinces was used only for sampling, and had no impact on the simulated NSOs. All of these maps were converted into HexSim spatial data input files comprised of 543,400 hexagons, with each hexagon being 86.6 ha in area and 1 km across (measured as the distance between parallel edges).

Our habitat and modeling region maps are described in detail in Appendix C of the U.S. Fish and Wildlife Service's 2011 Revised Recovery Plan for the NSO (USFWS 2011). NSO habitat is often subdivided into distinct components including nesting, roosting, foraging, and dispersal habitats. Nesting–roosting habitat is also suitable for foraging and dispersal, whereas foraging and dispersal habitats provide only for those functions. As our intent was to accurately capture the relative suitability of breeding habitat for NSOs, we modeled nesting–roosting and foraging (NRF) habitat, but not dispersal habitat. We used information from a literature review and expert opinion to develop a series of alternative models of forest condition corresponding to NRF habitat within each modeling region.

We used MaxEnt (Phillips et al. 2008, Phillips and Dudik 2008) to model relative habitat suitability, and tested the effectiveness of our results using cross-validation. We first identified the best NRF habitat models individually for each modeling region, and subsequently challenged them through the addition of precipitation, temperature, and climate variables (in an attempt to improve their predictive ability). Through this approach we identified relative habitat suitability (RHS) models that accurately and consistently discriminated among areas of varying suitability for spotted owls without over-fitting. Our RHS models were found to have good to excellent discrimination ability, to be well calibrated, and to have sufficient generality (USFWS 2011). These RHS models were evaluated at the 200 ha scale (i.e., covariate values from the 200 ha area around each pixel were used to estimate RHS of the focal pixel). MaxEnt assigned each 30×30 m raster pixel in the RHS map an integer weight between 0 (non-habitat) and 100 (optimal habitat).

Our HexSim habitat map was developed from the RHS data by intersecting it with the grid of 543,400 hexagonal cells. Each hexagon was assigned a score equal to the mean of the pixel values contained within it. These scores, which averaged the RHS data on a hexagon-by-hexagon basis, varied between 0.00 and 90.34. The RHS scores directly affected dispersal behavior, strongly influenced survival rates (through mechanisms discussed below), and indirectly affected reproduction.

Model parameters

Our NSOs had six separate traits that allowed individuals to be categorized into (i) four stage classes (fledgling, juvenile, sub-adult, and adult), (ii) three resource classes (low, moderate, and high), (iii) territory status (owner or floater), (iv) location, stratified by modeling region, (v) location, stratified by physiographic province, and (vi) BO exposure, which varied based on modeling region (USFWS 2011). The simulated NSOs interacted with the landscape through two related mechanisms. First, the owls attempted to construct relatively small non-overlapping territories, which played a role in regulating owl densities and in the determination of BO impacts. As is true in nature, not all NSOs were successful at territory establishment, and those who failed became non-breeding “floaters”, at least temporarily. Second, our simulated NSOs established large overlapping home ranges (the size varied by modeling region), which they used to acquire resources.

Simulated NSOs moved through the first three stage classes yearly. Individuals were placed into three resource classes based on their ability to acquire resources (RHS was a proxy for resources). This process involved resource acquisition targets, which are input parameters that varied by modeling region, and specified the amount of resource an unconstrained NSO would attempt to acquire. Changes in resource acquisition targets accounted for latitudinal differences in home range size (Gutiérrez et al. 1995). NSOs that acquired less than 1/3 of their resource target were assigned to the low resource class. Those who acquired 2/3 or more were assigned to the high resource class, and the remaining NSOs were put into the moderate class. Resources were acquired from simulated NSO home ranges, which were large and could overlap. Resource acquisition rates were thus emergent properties of the simulations that varied based on modeling region, home range size (which varied by modeling region), resource availability, and competition with neighboring NSOs (the resources available within a single hexagon were divided up equally among any NSO who included that hexagon in their home range).

Territory sizes were 2–3 hexagons, depending on the RHS values. This implied that defended areas were always 173 or 260 ha (see USFWS 2011). Territory construction was restricted to adjacent hexagons with

habitat scores of 35 or more (on a scale of 0–90.34), and all territories were required to have a minimum cumulative habitat score of 105, which was possible with two relatively high-value RHS hexagons, but more commonly required three adjacent hexagons.

The life cycle was 1 year in length. The year began with a survival event, with survival rates being a function of stage class, resource class, and BO presence–absence (see below). Next, each NSO’s age was incremented by one year. Then floaters (NSOs without territories) prospected for territories. Prospecting NSOs were allowed to search an area up to 500 hexagons, in hopes of identifying a suitable unoccupied territory. The search process was not random; instead, NSOs tended to gravitate towards better quality hexagons. Allowing NSOs to prospect over such a large area could potentially exaggerate the rate of successful territory establishment. However, the large prospecting area afforded the simulated NSOs some compensation for their relatively unsophisticated search strategy.

The next step in the NSO life cycle was to determine whether newly territorial NSOs were to be influenced by a BO, based on modeling region-specific encounter probabilities that varied from 0.18 to 0.71 (USFWS 2011). Our simulated NSOs never abandoned their territories (a simplification made for the sake of model parsimony), and the placement of NSOs into BO influence categories (present versus absent) was made just once for each territory-holding NSO, immediately after territory establishment. Non-territorial NSOs were assumed to be unaffected by BOs. The BO encounter probabilities were based on the proportion of NSO territories in which BOs were detected on each of 11 demographic study areas (Robert Anthony, Katie Dugger, pers. comm.; see Forsman et al. 2011—Appendix B for details). The consequence for simulated NSOs of exposure to a BO was a lower survival rate (Table 1). Data describing BO impacts on NSO reproduction or site fidelity were not available range-wide, and these feedbacks were therefore not included in the model.

The reproductive pulse followed the assignment of BO impacts. Because our model was of females only, we used empirically-derived fecundities (Forsman et al. 2011) to parameterize reproduction. There was no mortality between the reproduction and dispersal events, so the fecundities could be interpreted as numbers of fledglings per territorial female. We used

Table 1 Survival rates of NSOs in relation to stage class, habitat quality (resource class), and presence-absence of barred owls

Stage class	Resource class	Survival rate without barred owls	Survival rate with barred owls
Stage 0	Low	0.366	0.280
	Medium	0.499	0.413
	High	0.632	0.546
Stage 1	Low	0.544	0.458
	Medium	0.718	0.632
	High	0.795	0.709
Stage 2	Low	0.676	0.590
	Medium	0.811	0.725
	High	0.866	0.780
Stage 3	Low	0.819	0.733
	Medium	0.849	0.763
	High	0.865	0.779

fecundity values of 0, 0.070, 0.202, and 0.333 for stage classes 0–3, respectively. HexSim's reproduction event is parameterized with probabilities for each integer clutch size. Clutches were limited to 0, 1, or 2 NSOs, and the clutch size probabilities were obtained from the fecundities under the assumption that, for any given stage class, clutches of size 1 and 2 were equally likely (Robert Anthony, pers. comm.).

After reproduction, the stage class 0 NSOs dispersed. Our dispersal event allowed these fledglings to move a maximum of 250 hexagons. The fledglings would stop dispersing if they encountered a habitat patch that could qualify as a territory. Dispersing NSOs were assigned moderate spatial autocorrelation, and tended to avoid poor quality habitats. The process of territory establishment (described above) imposed limited density-dependence upon the NSO population. In contrast, dispersal frequency and behavior were completely unaffected by the presence of conspecifics, thus intentionally ignoring density-dependent emigration. This simplification reduced the number of variables, and ensured that observed source-sink structure (e.g. relationship to habitat quality) was not a necessary consequence of the model parameterization.

The simulation year ended with territorial NSOs establishing home ranges, and acquiring resources from them. Simulated home range sizes varied by modeling region based on estimates from a number of

field studies (see summary in Schilling 2009). We used the largest observed home range size estimates to parameterize HexSim, because the simulated NSOs were not obligated to extract resources from the entire area. Simulated NSOs simply had the potential to acquire resources over large areas if doing so was necessary to meet their resource target. Unlike territories, home ranges could overlap, and the resources they contained were shared equally. This made intraspecific exploitative competition possible.

Survival rates were based on empirical estimates obtained principally from long-term demographic study areas (DSAs) located within the modeling regions. Stage class 0 survival estimates were taken from (Franklin et al. 1999, pp. 27, 28). Forsman et al. (2011) provided stage class-specific survival estimates for each of 11 DSAs, with mean apparent survival values for stage 1–3 males and females listed separately. We computed the mean of each pair (males and females) and identified the smallest and largest of these mean values. For any given stage class, the smallest mean value was assigned to individuals in the low resource class. Likewise, the largest stage-specific mean value was assigned to individuals in the high resource class. The stage-specific survival rates for individuals in the medium resource class were set equal to the mean taken over all of the survival estimates for that stage class. Through this process, survival rates were obtained for stage 0–3 NSOs in all three resource classes (Table 1).

Finally, a complementary set of stage-specific coefficients were generated that reduced NSO survival rates to account for the impact of BOs (Table 1). The magnitude of this effect was based on the best meta-analysis model for survival with an additive BO covariate across all DSAs (Forsman et al. 2011).

Environmental stochasticity

Our results are based principally on ten replicate simulations that did not include environmental stochasticity. However, for comparison purposes, we ran 100 additional replicates that included an environmental stochasticity scheme developed for use in the US Fish and Wildlife Service's recovery planning (USFWS 2011). Our stochastic HexSim NSO model drew survival and reproduction rates randomly from a collection of values, with survival and reproduction being uncorrelated (Robert Anthony, pers. Comm.).

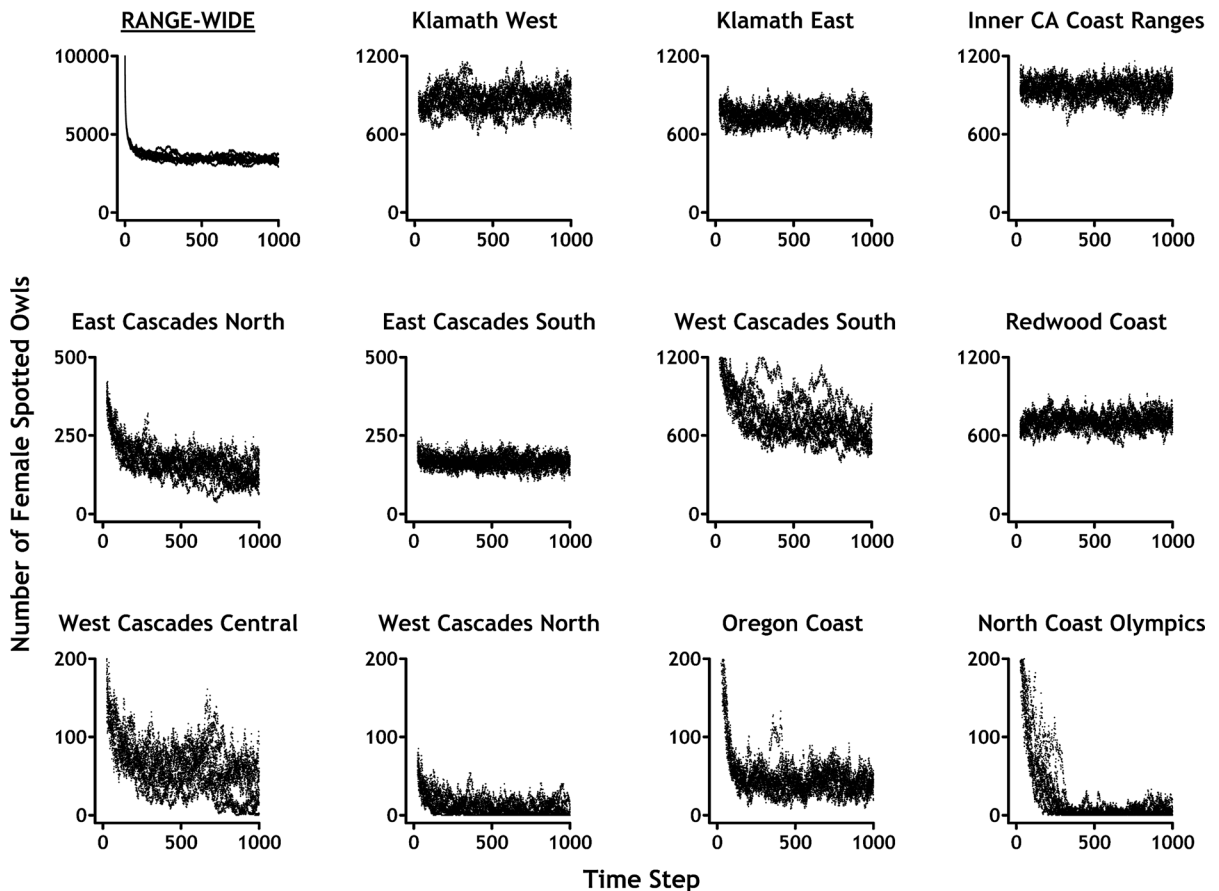


Fig. 1 The simulated NSO population size, stratified by modeling region. The results from ten separate replicates are shown. The vertical axis maximum varies between plots. These results are from simulations that did not include environmental stochasticity

Stochastic survival rates were obtained by multiplying each of the original rates (Table 1) by a single coefficient drawn randomly each year from the set {0.975, 0.980, 0.985, ..., 1.015, 1.020, 1.025}. Stochastic reproductive rates were obtained by multiplying each of the original fecundities (described above) by a single coefficient drawn randomly each year from the set {0.5, 1.0, 1.5}.

Model calibration

The principal metric used to evaluate the model was population size, tracked range-wide, per modeling region (Fig. 1), and also per DSA. The model's performance was assessed in part by comparing all three measures of simulated population size to field data. Not all DSAs had data that could be used to

approximate the density of female NSOs, and for calibration purposes, the following eight were selected: Cle-Elum, Olympic, Oregon Coast, HJ Andrews, Tyee, Klamath, Cascades, and Hoopa. Discrepancies in the fit between simulated and observed population size were addressed by varying the resource targets (described above).

Dispersal is a critical process through which landscape attributes impact NSO population size and metapopulation structure, and is a primary concern in habitat conservation network design (Murphy and Noon 1992). Estimates of true natal dispersal distances were made from movements of banded NSOs (Table 2 and Fig. 9 in Forsman et al. 2002), and compared to model output. HexSim dispersal parameters were modified until a close fit to the empirical data was obtained.

Model output

Our principal simulation products were “rate-based” and “count-based” matrices, in which every row and column represented a modeling region or a physiographic province. The count-based matrices recorded the actual numbers of individuals moving between locations (referred to below as “flux”). Our rate-based matrices, which are analogous to the “connectivity matrix” of Jacobi and Jonsson (2011), were obtained by dividing these counts by the simulated location-specific occupancy rates. We used the count-based matrices to both quantify emigration and immigration frequency (using row and column sums), and to measure Net Flux, a metric we describe below. Source-sink performance was set equal to the difference between the emigration and immigration counts, with net exporters labeled sources, and net importers labeled sinks (tallying births minus deaths produced virtually identical results, likely because the model was at steady state when the data was collected). We used the rate-based matrices to measure how changes in connectivity affected lambda (the matrix’s dominant eigenvalue) and thus population growth rate.

If $C_{row, col}$ represents a count-based matrix, then $Net\ Flux(A,B) = C_{B,A} - C_{A,B}$ describes the quantity $Flux(A \rightarrow B) - Flux(B \rightarrow A)$, where A and B represent individual locations (in our case modeling regions or physiographic provinces). We also refer to a metric “ $\Delta\lambda$ ” that here represents the change in overall population growth rate that would result from severing the connection between two locations without altering the flux in the reverse direction. Specifically, we compute $\Delta\lambda(A, B)$ as $(\lambda^M - \lambda^O) / \lambda^O$, where λ^O is the dominant eigenvalue of the original rate-based matrix and λ^M is the dominant eigenvalue of the modified rate-based matrix obtained from adding $Pr(A \rightarrow B)$ to $Pr(A \rightarrow A)$, and then setting $Pr(A \rightarrow B)$ to zero. Hence, $\Delta\lambda(A, B)$ measures the cost of prohibiting any movement from A to B , forcing those individuals instead to remain in location A . Defined this way, $\Delta\lambda$ will be positive when the change in flux increases the population growth rate, and will be negative when the growth rate decreases. The $\Delta\lambda$ values can be small, and for convenience we report them as a relative value, $\Delta\lambda^R$, defined as the percent of the maximum observed absolute value. $\Delta\lambda^R$ necessarily ranges between $\pm 100\%$. Our use of $\Delta\lambda$ values mirrors the application

of eigenvalue perturbation theory in Jacobi and Jonsson (2011).

Results

Our simulations produced a steady-state range-wide population size of roughly 3,400 female NSOs. Regional population sizes (Fig. 1) vary from low in the north, especially the northwest (e.g., <100 in the North Coast Olympics and West Cascades North modeling regions), to high in parts of southern Oregon and northern California (e.g. >750 in the Inner California Coast, Klamath East, Klamath West, Redwood Coast, and West Cascades South modeling regions). Differences in the observed versus simulated number of female spotted owls on the eight DSAs identified in the Model Calibration section ranged from 5 to 47 %, with a mean absolute percentage difference of 26 % (USFWS 2011).

Most modeling regions and physiographic provinces functioned as demographic sinks (Table 2). The addition of environmental stochasticity altered the source-sink classification in just one modeling region (West Cascades South), and no provinces. The addition of environmental stochasticity caused the relative source-sink strength (Table 2) to change in excess of 50 % in just one modeling region (West Cascades South) and one province (Oregon Western Cascades). The spatial distribution of sources and sinks appeared to vary depending on whether they were tracked by modeling regions or physiographic provinces (Fig. 2). The northern portions of the NSO’s range functioned as a blend of seemingly mild sinks and mediocre sources, due largely to low occupancy rates. The central and southern portions of the range tended to experience higher population sizes, and had more pronounced source-sink activity. The individual modeling regions and physiographic provinces were large enough to contain multiple distinct source and sink areas, and additional sampling schemes composed of smaller spatial units could be used to reveal this fine-grain structure. Our methodology ensured that source-sink properties varied along a continuum, with source and sink strength influenced by the size, shape, and location of individual habitat sampling units. This approach also gives rise to pseudo-sinks (Watkinson and Sutherland 1995; Dias 1996). When excess immigration causes NSO densities in source

Table 2 Observed source and sink attributes of the regions and provinces

Location	Map index	Percent of population (standard)	Source–sink type (standard)	Source–sink type (stochastic)	Source–sink strength (standard)	Source–sink strength (stochastic)
Modeling Regions						
East Cascades south	R9	3.8	Sink	Sink	100	100
Oregon coast	R5	1.0	Sink	Sink	48.7	49.8
Redwood coast	R10	16.4	Sink	Sink	28.1	33.6
West Cascades central	R4	1.2	Sink	Sink	16.9	20.8
North coast Olympics	R1	0.1	Sink	Sink	3.6	4.1
West Cascades north	R2	0.1	Sink	Sink	3.5	3.7
West Cascades south	R6	15.3	Source	Sink	25.8	5.7
East Cascades north	R3	3.3	Source	Source	31.7	33.8
Klamath west	R7	20.0	Source	Source	51.1	30.7
Inner California coast ranges	R11	21.7	Source	Source	97.9	100
Klamath east	R8	17.1	Source	Source	100	67.3
Physiographic Provinces						
California coast range	P10	16.6	Sink	Sink	100	100
Oregon eastern Cascades	P8	3.5	Sink	Sink	46.8	29.4
Oregon coast range	P5	0.8	Sink	Sink	41.8	29.8
California Cascades	P12	2.8	Sink	Sink	35.9	39.4
Washington western Cascades	P2	1.3	Sink	Sink	7.2	7.0
Oregon Willamette Valley	P6	>0.0	Sink	Sink	6.2	3.7
Washington western lowlands	P4	>0.0	Sink	Sink	3.3	2.7
Washington Olympic Peninsula	P1	>0.0	Sink	Sink	0.1	0.0
Washington eastern Cascades	P3	1.6	Source	Source	4.6	5.0
Oregon western Cascades	P7	23.3	Source	Source	37.1	18.3
Oregon Klamath	P9	13.7	Source	Source	37.6	26.9
California Klamath	P11	36.4	Source	Source	100	100

Map Index values correspond to those in Fig. 2. The right two columns express source-sink strength as a percent of the best source or worst sink. Data in the columns labeled “Standard” were obtained from the simulations that did not include environmental stochasticity

populations to increase beyond local carrying capacities, habitat and demographic limitations emerge within pseudo-sink populations, causing them to behave like sinks. Our methodology does not specifically identify pseudo-sinks (though this could be done by generating output matrices for snapshots in time, which the model permits).

We used two simple linear regressions to examine how effectively habitat quality predicted the observed source-sink properties. For each region and province, we calculated the mean habitat suitability (RHS) of its hexagons and recorded the source-sink strength as a percentage of the worst sink (−100 to 0) or best source (0 to 100). Both regression analyses revealed non-significant relationships between habitat suitability and source-sink strength ($r^2 = 0.18$, $F = 1.98$, $P = 0.19$ for modeling regions; $r^2 = 0.14$, $F = 1.57$, $P = 0.24$ for provinces). These weak relationships reflect multiple complicating factors including habitat fragmentation, intraspecific exploitative competition, the impact of BOs on NSO survival, strict NSO site fidelity, and mechanistic movement behavior. Recall that our source-sink properties emerge from interactions between individuals and the landscape. This contrasts with traditional models in which landscape source-sink properties are stipulated in advance (based on habitat quality), and used explicitly to guide the redistribution of individuals.

Net Flux between modeling regions was greatest from the Klamath East to East Cascades south modeling regions (Table 3), and between the California Klamath and California Coast Range physiographic provinces. Net Flux was strongly correlated with $\Delta\lambda$, but the impact of severing $Flux(A \rightarrow B)$ versus $Flux(B \rightarrow A)$ varied considerably (Table 3), indicating that the flux in a specific direction was sometimes particularly important to the population. In an evaluation of the simulations performed without environmental stochasticity, we found that in the regions and provinces respectively, 79 and 85 % of the variation in $\Delta\lambda$ was explained by Net Flux (based on the entire data set, not the subset displayed in Table 3). The addition of environmental stochasticity had little impact on Net Flux or $\Delta\lambda$.

The worst sink regions were R5 and R9, and the best source regions were R8 and R11. R9 and R5 were also the recipients of the two largest Net Flux values, and neither made a net contribution to any other modeling region. R11 and R8 both contributed

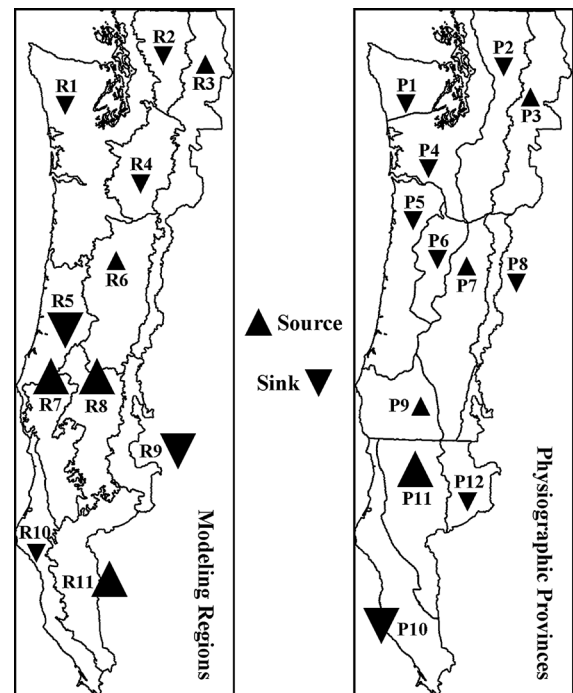


Fig. 2 A graphical presentation of the relative source and sink values displayed in Table 2. The larger symbols denote sources or sinks that exceeded 50 % of the maximum observed value. The R and P values correspond to the Map Index column in Table 2. These results are from simulations that did not include environmental stochasticity

substantially to other regions. R11 supported three regions to the north, and its flux to R7 was the third largest overall. R8 supported R6 and R9, with the Net Flux to R9 being the largest observed. R8's capacity to export NSOs was apparently buoyed by it also being a net importer from both R7 and R11. A similar pattern emerged from the physiographic provinces. P10 and P8, the worst two observed sinks, were the recipients of the largest Net Fluxes of NSOs, and neither was a significant net exporter. P11 and P9, the two best sources, both exported NSOs to their neighboring provinces. The three best source modeling regions, R11, R8, and R7, were also responsible for the largest observed Net Flux values. In fact, every substantially positive Net Flux of NSOs (stratified both by regions and provinces) emanated from a demographic source.

Our results reveal two principal zones of simulated NSO productivity (Fig. 3). The largest net landscape-scale flux originates in the California Klamath, and it distributes NSOs primarily into the California coast range and the California cascades (Fig. 3, bottom oval).

Table 3 Net Flux and $\Delta\lambda^R$ for the regions and provinces exhibiting a Net Flux of at least 10 % of the maximum observed value

Starting region	Ending region	% Net flux (standard)	% Net flux (stochastic)	$\Delta\lambda^R$ (standard)	$\Delta\lambda^R$ (stochastic)
Modeling Regions					
Klamath east	East Cascades south	100	100	85.1 [−100]	74.7 [−100]
Klamath west	Oregon coast	49.5	49.2	45.9 [−54.4]	39.7 [−50.5]
Inner California coast ranges	Klamath west	44.4	71.6	28.3 [−21.0]	41.2 [−31.0]
Klamath west	Redwood coast	36.2	43.6	3.9 [−4.5]	−2.9 [3.1]
Klamath east	West Cascades south	36.0	42.5	27.4 [−44.7]	31.3 [−52.4]
Inner California coast ranges	East Cascades south	30.4	32.8	22.4 [−14.2]	21.6 [−14.6]
West Cascades south	Oregon coast	28.7	24.5	8.6 [−1.4]	5.4 [−0.9]
West Cascades south	East Cascades south	27.8	13.4	24.4 [−19.5]	12.1 [−10.4]
East Cascades north	West Cascades central	21.8	25.4	20.9 [−36.8]	21.9 [−30.1]
Inner California coast ranges	Klamath east	19.7	28.3	18.4 [−15.2]	24.2 [−20.8]
Klamath west	Klamath east	12.7	21.8	19.1 [−19.5]	24.9 [−28.9]
East Cascades north	West Cascades south	4.7	14.4	−26.4 [1.8]	55.0 [−2.4]
Physiographic Provinces					
California Klamath	California coast range	100	100	47.4 [−100]	45.2 [−100]
Oregon western Cascades	Oregon eastern Cascades	52.9	34.2	18.6 [−37.6]	11.2 [−25.7]
Oregon Klamath	Oregon western Cascades	35.0	29.4	14.7 [−18.1]	11.3 [−15.4]
Oregon western Cascades	Oregon coast range	22.9	15.3	4.1 [−0.9]	2.4 [−0.6]
California Klamath	California Cascades	22.2	25.9	12.6 [−27.0]	12.8 [−26.3]
Oregon Klamath	Oregon coast range	19.2	14.7	10.2 [−10.4]	7.2 [−7.7]
California Klamath	Oregon Klamath	8.0	11.2	6.6 [−8.8]	6.4 [−10.3]

The Net Flux and $\Delta\lambda^R$ values are expressed as a percent of the maximum absolute (either positive or negative) observed value. The $\Delta\lambda^R$ values for the flux in the opposite direction are shown in brackets. Negative $\Delta\lambda^R$ values result from matrix manipulations that decrease λ (e.g. trapping individuals in a sink). Data in the columns labeled “Standard” were obtained from the simulations that did not include environmental stochasticity

The second principal net flux begins in the Oregon Klamath, and it extends to the north, moving NSOs into the Oregon coast range and the Oregon cascades. While these results are not surprising, there would be no way to draw such conclusions from the traditional products of spatially explicit population models, such as the population trends displayed in Fig. 1.

Our estimates of source-sink properties and Net Flux can be used to construct a summary graph (Fig. 4). Range-wide, one-third of the NSO population is living in demographic sinks, some of which appear more dependent on sources than others. The California and eastern Oregon Cascades, for example support roughly equal fractions of the simulated population. Yet the eastern Oregon Cascades absorb many more simulated NSOs, suggesting this region could at present be a net liability. The Klamath region appears the most critical to population stability overall (Fig. 4).

Discussion

Individual-based models are commonly used to develop population viability analyses (PVA) for species conservation efforts. But estimates of future population size or probabilities of extinction—the typical products of a PVA model—cannot reveal what role specific landscape locations play in promoting species viability. This study of NSO population dynamics shows how additional insights can be obtained from such a model. We used a detailed spatially-explicit IBM to generate location-stratified matrices, and used the matrices to evaluate species–landscape interactions. Our analysis illustrated how demographic sources and sinks were distributed spatially, how this distribution drove immigration and emigration rates, and how altering these rates could have impacts range-wide. We replicated our

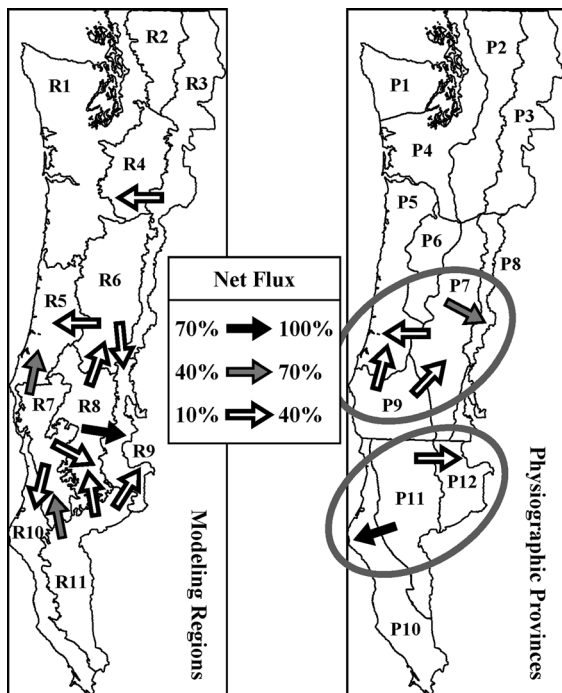


Fig. 3 A graphical representation of the Net Flux values listed in Table 3. The largest fluxes are displayed in *black*, intermediate values are shown in *gray*, and the smallest Net Flux values are shown in *white*. The *arrows* point in the direction of the flux. Two principle patterns of NSO flux that emerge from the simulations are most evident when resolved by the physiographic provinces (see *gray ovals*), but are also apparent within the regions. These results are from simulations that did not include environmental stochasticity

analysis using simulations incorporating environmental stochasticity, and by doing so were able to demonstrate that our results appear robust to model uncertainty. We drew our conclusions from simulations run within a static landscape, but our methodology could be employed, unchanged, in a dynamic environment.

We know from theory that it is critical to protect demographic sources, and that it can also be important to preserve or even improve some demographic sinks. Jacobi and Jonsson (2011) reinforced this point when they concluded that “the sites that act as both donor and recipient simultaneously are most important for the persistence of the population”. Our results (Fig. 4) lend additional support to this principle, though we make an added distinction between flux and Net Flux. Our methods can be used to illustrate how sources and sinks are arrayed across a landscape, and can do so at multiple spatial scales simultaneously. And these

estimates of source-sink behavior emerge as the product of ecologically-meaningful mechanisms that are built into the simulation model—they are not inferences based principally upon habitat pattern and dispersal kernels.

At steady-state, large Net Flux values suggest a dependency of one location upon another, and the population-wide significance of these relationships is reinforced by high correlations between Net Flux and $\Delta\lambda$. By locating dominant Net Flux values within the landscape (Fig. 3) we were able to identify two principle zones of spotted owl productivity. These maps could be used to infer how local management decisions could have range-wide consequences. For example, our results suggest that specific source (R7, R8, R11) and sink (R5 & R9) regions (Fig. 3) may be particularly important areas to target for habitat protection and restoration, respectively. Likewise, this analysis indicates that future landscape changes limiting dispersal between the Klamath and Inner California Coast Ranges might be more consequential for NSOs than analogous disturbances affecting movement between the Klamath and Redwood Coast (Fig. 4). The modeling regions and physiographic provinces are quite large, and additional analysis making use of multiple fine-grained sampling schemes would need to be performed before any actual management recommendations could be defended.

Conclusions

When habitat size and quality are poor predictors of population performance, complex source-sink dynamics are the likely culprit. The existence of complex source-sink dynamics may be more the rule than the exception, particularly for species of conservation concern. A theoretical foundation for understanding the landscape-scale implications of source-sink dynamics was constructed by Pulliam (1988). But it has proven difficult to develop methods that connect this theoretical work to the practical conservation applications that would surely benefit from it (Liu et al. 2011). Here, we have attempted to bridge this gap using the NSO as a case study, but have developed methodology that is broadly applicable to many species and landscapes. Importantly, our approach can reveal movement patterns and source-sink structures at multiple spatial scales without compromising

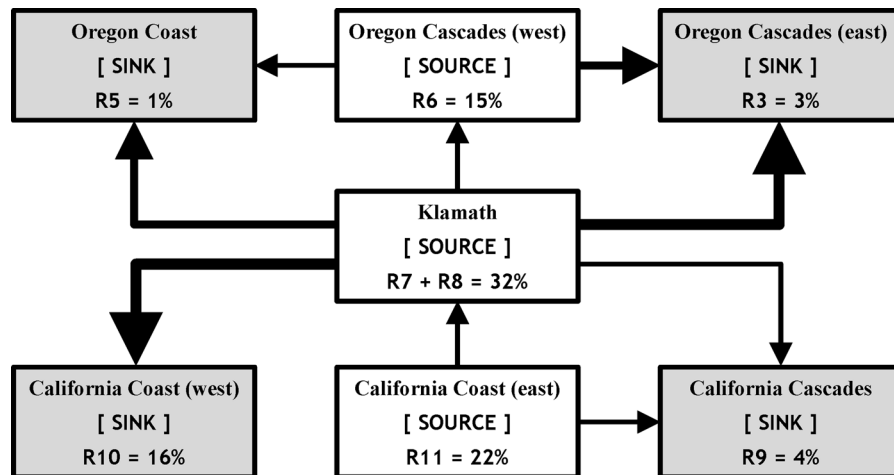


Fig. 4 A schematic of important source-sink interdependencies, inferred qualitatively from the information in Tables 2 and 3. The *arrows* show the most important positive Net Fluxes, with the *thicker lines* indicating larger values. Sinks are displayed in *gray*, and sources in *white*. Mean occupancy,

corresponding to specific modeling regions, is shown at the bottom of each box as a percent of the total simulated population size. The Oregon Coast (R5) percent occupancy is low as this region does not extend north to the state boundary

the ecological sophistication of the model system. This complements other popular methodologies (Minor and Urban 2007; Phillips et al. 2008; Moilanen 2011; Rayfield et al. 2011; Carroll et al. 2012), which more precisely address connectivity, but at a cost to realism.

Our location-stratified projection matrix models are compact and easy to understand, and their derivation from the biologically realistic IBM imbues them with conservation relevance. Matrix models have the added advantage of being simple and familiar, and they facilitate rapid experimentation. Our manipulation of the rate-based matrices for the purpose of obtaining $\Delta\lambda_s$ serves as an example. While the IBM itself could have been used to quantify the range-wide population responses to changes in connectivity, setting up and running all of the simulations necessary to make independent assessments for every pair of modeling regions and physiographic provinces would be a daunting task. Performing the equivalent analysis using the projection matrix model is straightforward and efficient.

The approach described here unifies source-sink and landscape connectivity analyses, and does so without imposing methodological constraints on biological realism. Our results illustrate how individual sources and sinks interact to form networks, and they quantify the population-wide consequences of small-scale modifications to habitat connectivity. Our methodology will also help illustrate why simple

measures of habitat quality often turn out to be poor predictors of population performance. Extensions of this work could incorporate dynamic habitat maps depicting future land use, climate change effects, or other disturbance regimes.

Acknowledgments Our NSO simulation model could not have been developed without the invaluable assistance generously provided by Robert Anthony, Katie Dugger, Paul Henson, Brendon White, and Betsy Glenn. We are indebted to Robert Schooley, Barry Noon, and an anonymous reviewer for many detailed suggestions that greatly improved the manuscript. This work was supported in part by USFWS Agreements 134250BJ151 and F12AC01135 to JRD, and grants RC-1541 and RC-2120 to JL from the Strategic Environmental Research and Development Program. The information in this document has been funded in part by the U.S. Environmental Protection Agency. It has been subjected to review by the National Health and Environmental Effects Research Laboratory's Western Ecology Division and approved for publication. Approval does not signify that the contents reflect the views of the Agency, nor does mention of trade names or commercial products constitute endorsement or recommendation for use.

References

- Baguette M, Van Dyck H (2007) Landscape connectivity and animal behavior: functional grain as a key determinant for dispersal. *Landscape Ecol* 22:1117–1129
- Bunn AG, Urban DL, Keitt TH (2000) Landscape connectivity: a conservation application of graph theory. *J Environ Manage* 59:265–278

- Carroll C, McRae B, Brookes A (2012) Use of linkage mapping and centrality analysis across habitat gradients to conserve connectivity of gray wolf populations in western north America. *Conserv Biol* 26:78–87
- Courtney SP, Blakesley JA, Bigley RE, Cody ML, Dumacher JP, Fleischer RC, Franklin AB, Franklin JF, Gutiérrez RJ, Marzluff JM, Sztukowski L (2004) Scientific evaluation of the status of the northern spotted owl. Sustainable Ecosystems Institute, Portland
- Dias P (1996) Sources and sinks in population biology. *Tree* 11:326–330
- Dugger KM, Anthony RG, Andrews LS (2011) Transient dynamics of invasive competition: barred owls, spotted owls, habitat, and the demons of competition present. *Ecol Appl* 21:2459–2468
- Ferraz G, Nichols JD, Hines JE, Stouffer PC, Bierregaard RO, Lovejoy TE (2007) A large-scale deforestation experiment: effects of patch area and isolation on Amazon birds. *Science* 315:238–241
- Forsman ED, Anthony RG, Reid JA, Loschl PJ, Sovern SG, Taylor M, Biswell BL, Ellingson A, Meslow EC, Miller GS, Swindle KA, Thraillkill JA, Wagner FF, Seaman DE (2002) Natal and breeding dispersal of northern spotted owls. *Wildl Monogr* 149:1–35
- Forsman ED, Anthony RG, Dugger KM, Glenn EM, Franklin AB, White GC, Schwarz CJ, Burnham KP, Anderson DR, Nichols JD, Hines JE, Lint JB, Davis RJ, Ackers SH, Andrews LS, Biswell BL, Carlson PC, Diller LV, Gremel SA, Herter DR, Higley JM, Horn RB, Reid JA, Rockweit J, Schaberl J, Snetsinger TJ, Sovern SG (2011) Population demography of northern spotted owls. *Studies in Avian Biology*. Cooper Ornithological Society. University of California Press, Berkeley
- Franklin AB, Burnham KP, White GC, Anthony RG, Forsman ED, Schwarz CJ, Nichols JD, Hines JE (1999) Range-wide status and trends in Northern Spotted Owl populations. U.S Fish and Wildlife Service, Portland
- Goodwin B (2003) Is landscape connectivity a dependent or independent variable? *Landscape Ecol* 18:687–699
- Gutiérrez RJ, Franklin AB, LaHaye WS (1995) Spotted Owl (*Strix occidentalis*). In: Poole A, Gill F (eds) *The birds of north America No 179: life histories for the 21st century*. The Philadelphia Academy of Sciences and The American Ornithologists' Union, Washington, pp 247–257
- Hansen A (2011) Contribution of source-sink theory to protected area science. In: Liu J, Hull V, Morzillo AT, Wiens JA (eds) *Sources, Sinks and Sustainability*. Cambridge University Press, Cambridge, pp 339–360
- Heinrichs JA, Bender DJ, Gummer DL, Schumaker NH (2010) Assessing critical habitat: evaluating the relative contribution of habitats to population persistence. *Biol Conserv* 143:2229–2237
- Hudgens BR, Morris WF, Haddad NM, Fields WR, Wilson JW, Kuefler D, Jobe T (2012) How complex do models need to be to predict dispersal of threatened species through matrix habitats? *Ecol Appl* 22:1701–1710
- Jacobi MN, Jonsson PR (2011) Optimal networks of nature reserves can be found through eigenvalue perturbation theory of the connectivity matrix. *Ecol Appl* 21:1861–1870
- Koh I, Rowe HI, Holland JD (2013) Graph and circuit theory connectivity models of conservation biological control agents. *Ecol Appl* 23:1554–1573
- Kool J, Moilanen A, Treml EA (2013) Population connectivity: recent advances and new perspectives. *Landscape Ecol* 28:165–185
- Liu J, Hull V, Morzillo AT, Wiens JA (eds) (2011) *Sources, Sinks and Sustainability*. Cambridge University Press, Cambridge
- Marcot BG, Raphael MG, Schumaker NH, Galleher B (2013) How big and how close? Habitat patch size and spacing to conserve a threatened species. *Nat Resour Model* 26:194–214
- McKelvey K, Noon BR, Lamberson RH (1993) Conservation planning for species occupying fragmented landscapes: The case of the northern spotted owl. In: Kareiva PM, Kingsolver JG, Huey RB (eds) *Biotic interactions and global change*. Sinauer, Sunderland, pp 424–450
- McRae BH, Dickson BG, Keitt TH, Shah VB (2008) Using circuit theory to model connectivity in ecology, evolution, and conservation. *Ecology* 89:2712–2724
- Minor ES, Urban DL (2007) Graph theory as a proxy for spatially explicit population models in conservation planning. *Ecol Appl* 17:1771–1782
- Minor ES, McDonald RI, Treml EA, Urban DL (2008) Uncertainty in spatially explicit population models. *Biol Conserv* 141:956–970
- Moilanen A (2011) On the limitations of graph-theoretic connectivity in spatial ecology and conservation. *J Appl Ecol* 48:1543–1547
- Murphy DD, Noon BR (1992) Integrating scientific methods with habitat conservation planning: reserve design for northern spotted owls. *Ecol Appl* 2:3–17
- Noon BR, McKelvey K (1996) Management of the spotted owl: a case history in conservation biology. *Annu Rev Ecol Syst* 27:135–162
- Núñez TA, Lawler JJ, McRae BH, Pierce DJ, Krosby MB, Kavanagh DM, Singleton PH, Tewksbury JJ (2013) Connectivity planning to address climate change. *Conserv Biol* 27:407–416
- Phillips SJ, Dudik M (2008) Modeling of species distributions with Maxent: new extensions and a comprehensive evaluation. *Ecography* 31:161–175
- Phillips SJ, Williams P, Midgley G, Archer A (2008) Optimizing dispersal corridors for the Cape Proteaceae using network flow. *Ecol Appl* 18:1200–1211
- Pulliam RH (1988) Sources, sinks, and population regulation. *Am Nat* 132:652–661
- Rayfield B, Fortin MJ, Fall A (2011) Connectivity for conservation: a framework to classify network measures. *Ecology* 92:847–858
- Schilling JW (2009) Demography, home range, and habitat selection of northern spotted owls in the Ashland Watershed. MS Thesis, Oregon State University
- Schumaker NH (2013) HexSim Version 2.5. U.S. Environmental Protection Agency, Environmental Research Laboratory, Corvallis, Oregon, USA. <http://www.epa.gov/hexsim>
- Stronen AV, Schumaker NH, Forbes GJ, Paquet PC, Brook RK (2012) Landscape resistance to dispersal: simulating long-term effects of human disturbance on a small and isolated

- wolf population in southwestern Manitoba, Canada. *Environ Model Assess* 184:6923–6934
- Thomas JW, Forsman ED, Lint JB, Meslow EC, Noon BR, Verner JA (1990) A conservation strategy for the northern spotted owl: report to the interagency scientific committee to address the conservation of the northern spotted owl. United States Government Printing Office, Washington
- USDA Forest Service and USDI Bureau of Land Management (1994) Record of decision for amendments to the forest service and bureau of land management planning documents within the range of the northern spotted owl: standards and guidelines for management of habitat for late-successional and old-growth forest related species within the range of the northern spotted owl. USDA Forest Service and USDI Bureau of Land Management, Portland, Oregon.
- USFWS (1990) Endangered and threatened wildlife and plants: determination of threatened status for the northern spotted owl. *Fed Reg* 55:26114–26194
- USFWS (2011) Revised recovery plan for the northern spotted owl (*Strix occidentalis caurina*). U.S. Fish and Wildlife Service, Portland
- Watkinson AR, Sutherland WJ (1995) Sources, sinks and pseudo-sinks. *J Anim Ecol* 64:126–130
- Wiens JD (2012) Competitive interactions and resource partitioning between northern spotted owls and barred owls in western Oregon. Dissertation, Oregon State University, Corvallis
- Yackulic CB, Reid JR, Davis R, Hines JE, Nichols JD, Forsman E (2012) Neighborhood and habitat effects on vital rates: expansion of the barred owl in the Oregon coast ranges. *Ecology* 93:1953–1966